View metadata, citation and similar papers at core.ac.uk
brought to you by CORE
provided by UPCommons. Portal del coneixement obert de la UPC

Reset control for DC-DC converters: an experimental application

Unnikrishnan Raveendran Nair, Ramon Costa-Castelló, and Alfonso Baños.

***Abstract*—Power converters in grid connected systems are required to have fast response to ensure the stability of the system. The standard PI controllers used in power converters are capable of fast response but with significant overshoot. In this paper a hybrid control technique for power converter using a reset $PI+CI$ controller is proposed. The $PI+CI$ controller can overcome the limitation of its linear counterpart (PI) and ensure a fast flat response for power converter. The design, stability and cost of feedback analysis for a DC-DC boost converter employing a $PI+CI$ controller is explored in this work. The simulation and experimental results which confirm the fast, flat response will be presented and discussed.**

***Index Terms*—Hybrid control, reset systems, energy systems, DC-DC converter, stability.**

I. Introduction

Reset controllers were first introduced by J C Clegg through the Clegg integrators (CI) for servo systems [1]. The CI is a hybrid dynamical system which resets its output to zero when input becomes zero providing improved performance and reduced overshoot. This was followed by many works involving different reset controllers like First Order Reset Elements (FORE) [2]–[6] and more recently $PI+CI$ controllers [7]–[9]. The reset controllers are capable of overcoming limitations of its linear counterparts and provide improved performance [10]. A general background on reset control systems can be obtained from the monograph [11].

The $PI+CI$ controller employs the CI along with a PI controller to improve its performance. The CI on its own is not able to ensure zero steady-state error unless there is an integrator in the plant. The $PI+CI$ uses integrator from PI controller to eliminate steady-state error and CI to achieve improved performance by allowing fast response with reduced overshoot. There has been many works done in the area of $PI+CI$ controllers involving laying out design criteria [8], [9] for different plants and stability analysis of such systems [7] [12] [13]. The application of such controllers in real world applications like pH in-line control [9], bilateral teleoperation [14], solar collector field [15], industrial wafer scanners [16] and control of industrial heat exchangers [17] have been explored.

Power converters in grid connected systems present an interesting field for the application of reset $PI+CI$ controllers. Modern grids are seeing increased penetration of renewable energy sources (RES) leading to an increased number of power converters in grids [18]. Power converter provide controllability over power supplied to grid, power conversion (DC↔AC) and matching of voltage levels [19], [20]. The non dispatchable nature of the power from RES has led to addition of electrical storage systems (ESS) in grid to ensure stable operation [21]. Power converters are again needed for grid connection of ESS. The motivation for using $PI+CI$ controllers for power converters stems from the need for these systems to respond to fast changes in load demands while maintaining the system parameters like voltage, frequency etc. within limits prescribed by grid codes. Sudden load changes can result in voltage flickers or tripping of electrical systems due to large frequency and voltage deviation if systems are not designed to respond quickly [22]. Currently most converters irrespective of the control method used, employ PI controllers as compensator for reference tracking. These PI controllers are tuned to have fast response to sudden reference change arising from load variations, to maintain grid parameters within prescribed limits. Though PI controllers are capable of such fast response they can have significant overshoot in their transient period highlighting a scope for improvement. As such $PI+CI$ reset controller can be a better choice for such systems with its ability of reduced overshoot. $PI+CI$ controllers are also capable of producing a fast flat response for first order plants [9]. This is an important attribute of the $PI+CI$ which can be exploited in converter control.

Many control techniques have been used in power converters to obtain flat response like, higher order sliding mode controls [23]–[25] and differential flatness theory [26]. Nevertheless, these controllers tend to be more complex in implementation. The $PI+CI$ is a simple modification of PI controller which can be easily implemented, designed with simple analytical equations and provide improved performance. As far as the authors' knowledge goes the use of such control in power converters have not been explored before.

This work proposes the implementation of $PI+CI$ reset controller for a DC-DC boost converter. The proposed work is an extension of [27] where applicability of reset control in DC-DC converters with ideal averaged converter models where studied. In this work the scope has been broadened with focus on designing for a generic converter model, experimental implementation of the proposed control, establishment of

Unnikrishnan Raveendran Nair and Ramon Costa-Castelló are with Institut de Robòtica i Informòtica industrial, Universitat Politècnica de Catalunya, 08034 Barcelona, Spain, (e-mail: uraveendran@iri.upc.edu, ramon.costa@upc.edu)

Alfonso Baños is with the Departmento Informática y Sistemas, Universidad de Murcia, 30100 Murcia, Spain,(e-mail: abanos@um.es)

This work is done as part of project which has received funding from the European Union's Horizon 2020 research and innovation programme under the Marie Skłodowska Curie grant agreement No 675318 (INCITE). This work is supported by the Spanish State Research Agency through the Mara de Maeztu Seal of Excellence to IRI (MDM-2016-0656) and Government of Spain under project DPI2016-79278-C2-1-R.

formal stability and robustness to: measurement, switching noise and parameter uncertainty. The implementation results will be presented and discussed here.

The rest of the paper is organised as follows. Section II introduces preliminaries like $PI + CI$ controller model, the reset control systems model, stability conditions and converter models employed. Section III shows the controller design for the proposed DC-DC boost converter, stability analysis, robustness under parameter uncertainty and cost of feedback analysis based on describing functions. Section IV presents the implementation and results obtained from lab along with simulation results. Finally, conclusion and scope for future work will be presented in Section V.

II. Preliminaries

A. Reset controller

After the seminal works introducing the CI and the FORE, general single-input single-output reset controllers derived from linear and time invariant base system, were introduced in the late 90's (see [11], [28] and references therein). In [5], the CI and the FORE are reformulated using the hybrid inclusions framework of [29], with a resetting law based on a sector condition over their input-ouput pairs. This modelling has been followed in many subsequent works including some generalizations, for example the model given in [30], which will be adopted in this work. A reset controller $\mathcal{R}$ is given by

$$\mathcal{R} = \begin{cases} \dot{\mathbf{x}}_r & = \mathbf{A}_r\mathbf{x}_r + \mathbf{B}_r e, \quad if(e, -u_{\mathcal{R}}) \in \mathcal{F} \\ \mathbf{x}_r^+ & = \mathbf{A}_\rho \mathbf{x}_r, \quad if(e, -u_{\mathcal{R}}) \in \mathcal{J} \\ -u_{\mathcal{R}} & = \mathbf{C}_r\mathbf{x}_r \end{cases} \tag{1}$$

where $\mathbf{x}_r \in \mathbb{R}^{n_r}$, $\mathbf{A}_r, \mathbf{B}_r$ and $\mathbf{C}_r$ are the appropriate system matrices and $-u_{\mathcal{R}}$ is the output of the reset controller employed. $\mathcal{F}, \mathcal{J}$ are the flow and jump sets of the system respectively. In the set defined by $\mathcal{F}$ the controller states flow according to linear differential equation whereas the states undergo a jump at the set $\mathcal{J}$. $\mathbf{x}_r^+$ represents the state of the controller after jump caused by the reset instance. The matrix $\mathbf{A}_\rho$ is the reset matrix which defines the system states after the reset instance. The flow set $\mathcal{F}$ is given by

$$\mathcal{F} = \{(e, -u_{\mathcal{R}}) \in \mathbb{R}^2 | e u_{\mathcal{R}} \leq -\frac{1}{\alpha} u_{\mathcal{R}}^2\} \tag{2}$$

while $\mathcal{J}$ is given by

$$\mathcal{J} = \{(e, -u_{\mathcal{R}}) \in \mathbb{R}^2 | e u_{\mathcal{R}} \geq -\frac{1}{\alpha} u_{\mathcal{R}}^2\} \tag{3}$$

where $\alpha > 0$ is as shown in Fig.1a The flow and jump sets defined using the above equations can be illustrated in a two dimensional plane as sectors shown in Fig.1a. The jump condition occurs along the boundary of $\mathcal{F}$ and $\mathcal{J}$ in Fig.1a [30]. The general reset controller expression in (1) can be used to express all the different reset controllers. For a detailed exposition to the hybrid inclusions framework, including definition of hybrid time and the solution concept for reset systems, the reader is referred to [29].

The PI+CI controller considered in this work is obtained by introducing a CI along with the classical PI controller and

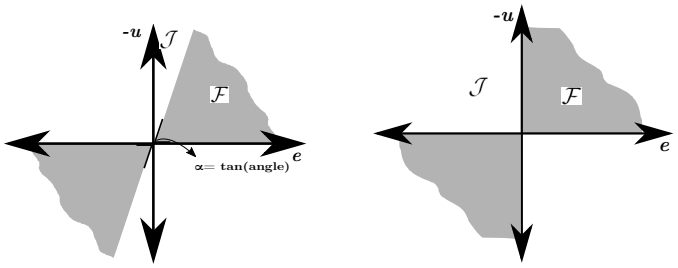

(a) General reset system (b) Clegg integrator(CI)

Fig. 1: (a), Sector condition for general reset controller. (b), Sector condition for CI with $\alpha \to \infty$.

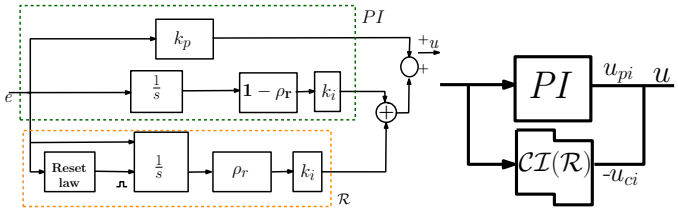

(a) (b)

Fig. 2: (a), PI+CI controller schematic.(b), An equivalent representation of PI+CI with $\mathcal{R}$ representing CI

is schematically represented as in Fig.2. The orange square region in Fig.2a represents the CI part and the green region represents the PI part. The reset law in CI part is defined by the boundary of $\mathcal{J}$ with $\mathcal{F}$. The term ρ_r is the reset ratio and represents the percentage of the total integral action that gets reset through the CI. For example, if $\rho_r = 0$ it results in a classic PI controller, which will be referred henceforth as PI_{base}, whereas a $\rho_r = 1$ results in P+CI controller. Once the PI_{base} controller has been designed, usually to obtain a fast response, the PI+CI controller acts by removing (or minimizing) the overshoot (and hence the significance of negative output of reset part). The desired design specification (a fast response without overshooting) may be obtained simply by adjusting the parameter ρ_r. As such, in this work, the design problem will be to find a ρ_r value between 0 and 1 which will ensure a flat response and an improved performance over PI controller.

The PI+CI controller [8] can be modelled as in (1) using:

$$\begin{cases} \dot{\mathbf{x}}_r & = \mathbf{A}_r\mathbf{x}_r + \mathbf{B}_r e, \quad if(e, -u_{ci}) \in \mathcal{F} \\ \mathbf{x}_r^+ & = \mathbf{A}_\rho \mathbf{x}_r, \quad if(e, -u_{ci}) \in \mathcal{J} \\ u & = \mathbf{C}_r(\rho_r)\mathbf{x}_r + \mathbf{D}_r e \end{cases} \tag{4}$$

where $\mathbf{x}_r = [x_i \ x_{ci}]^T$ are the states of the controller defined by the integrator (x_i) and CI (x_{ci}) states, and

$$\mathbf{A}_r \triangleq \begin{bmatrix} 0 & 0 \\ 0 & 0 \end{bmatrix}, \quad \mathbf{B}_r \triangleq \begin{bmatrix} 1 \\ 1 \end{bmatrix}, \quad \mathbf{C}_r \triangleq k_i \begin{bmatrix} 1-\rho_r & \rho_r \end{bmatrix}$$
$$\mathbf{D}_r \triangleq k_p, \quad \mathbf{A}_\rho \triangleq \begin{bmatrix} 1 & 0 \\ 0 & 0 \end{bmatrix} \tag{5}$$

Note that the dependence of $\mathbf{C}_r$ on ρ_r has been explicitly shown in (4),(5). The sets $\mathcal{F}$ and $\mathcal{J}$ for the PI+CI controller are defined as in (2, 3), where $\alpha > 0$ typically takes a large value

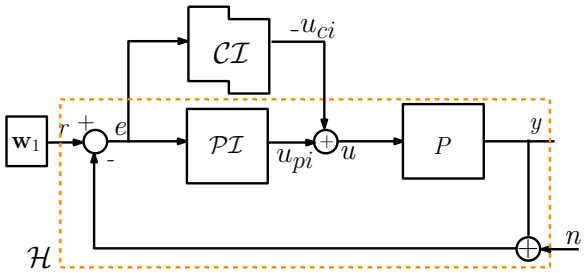

Fig. 3: Reset control system with a PI+CI controller and exogenous inputs in reference $\mathbf{w}_1$ and measurement noise n

(note that for $\alpha \to \infty$ the CI developed in [5] is recovered and this PI+CI controller is equivalent to that developed in [8], as far as its initial conditions are taken in the set $\mathcal{F}$); $-u_{ci}$,u_{pi} is output of CI, PI part respectively and u the output of PI+CI as shown in Fig.2b. The resulting $\mathcal{F}$ and $\mathcal{J}$ for PI+CI is represented as in Fig.1b. Although the PI+CI controller can also be built using a variable ρ_r , see [9], for the purposes of this work ρ_r will be a constant parameter.

B. Reset control as a hybrid dynamical system

The Fig.3 shows a general reset control system employing a $PI+CI$ controller. The reference to the system is represented by the exogenous signal $\mathbf{w}_1$ in Fig.3. It is assumed that $\mathbf{w}_1$ is a Bohl function and is represented as

$$\begin{aligned} \dot{\mathbf{w}}_1 &= \mathbf{A}_1\mathbf{w}_1, \mathbf{w}_1(0) = w_{10} \\ r &= \mathbf{C}_1\mathbf{w}_1 \end{aligned} \tag{6}$$

where $\mathbf{w}_1 \in \mathbb{R}^{n_1}$. As this work considers a reference tracking problem the disturbance inputs are not considered here. The additive input in the feedback path of Fig.3 represents the measurement noise, n. The plant (P) under consideration is represented in the state-space form as

$$\begin{aligned} \dot{\mathbf{x}}_p &= \mathbf{A}_p\mathbf{x}_p + \mathbf{B}_p u, \\ y &= \mathbf{C}_p\mathbf{x}_p \end{aligned} \tag{7}$$

where $\mathbf{x}_p \in \mathbb{R}^{n_p}$.

Therefore, using (4), (6), (7) the closed-loop system can be represented by (note that ρ_r is a constant parameter, explicit dependence on is shown)

$$\begin{cases} \dot{\mathbf{x}} &= \mathbf{A}(\rho_r)\mathbf{x}, & \mathbf{x} \in \mathcal{F}_\mathcal{C} \\ \mathbf{x}^+ &= \mathbf{A}_R\mathbf{x}, & \mathbf{x} \in \mathcal{J}_\mathcal{C} \\ y &= \mathbf{C}\mathbf{x} \end{cases} \tag{8}$$

where $\mathbf{x} \in \mathbb{R}^{n_p+2+n_1}$ is the state of closed loop system defined by $[\mathbf{x}_p, \mathbf{x}_r, \mathbf{w}_1]^T$. The matrices $\mathbf{A}$,$\mathbf{C}$,$\mathbf{A}_R$ are defined as

$$\mathbf{A}(\rho_r) \triangleq \begin{bmatrix} \mathbf{A}_p - \mathbf{B}_p\mathbf{D}_r\mathbf{C}_p & \mathbf{B}_p\mathbf{C}_r(\rho_r) & \mathbf{B}_p\mathbf{D}_r\mathbf{C}_1 \\ -\mathbf{B}_r\mathbf{C}_p & \mathbf{A}_r & \mathbf{B}_r\mathbf{C}_1 \\ 0 & 0 & \mathbf{A}_1 \end{bmatrix} \tag{9}$$

$$\mathbf{C} \triangleq (\mathbf{C}_p\ \mathbf{0}_2\ \mathbf{0}_{n1}), \quad \mathbf{A}_R \triangleq diag(\mathbf{I}_{n_p}, \mathbf{A}_\rho, \mathbf{I}_{n_1})$$

where $\mathbf{I}$ is unit matrix and $\mathbf{0}$ is a zero vector of appropriate order. The set $\mathcal{F}_\mathcal{C}, \mathcal{J}_\mathcal{C}$ is the same as that in (2)-(3) but reformulated as a function of system states given by

$$\mathcal{F}_\mathcal{C} = \{\mathbf{x} \in \mathbb{R}^{n_p+2+n_1} | \mathbf{x}^T\mathcal{M}\mathbf{x} \leq 0\} \tag{10}$$

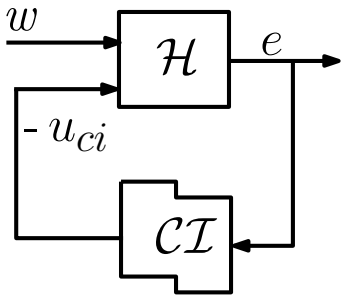

Fig. 4: Reduced feedback interconnection from Fig.3 of LTI dynamical system ($\mathcal{H}$) and CI controller.

while $\mathcal{J}$ is given by

$$\mathcal{J}_\mathcal{C} = \{\mathbf{x} \in \mathbb{R}^{n_p+2+n_1} | \mathbf{x}^T\mathcal{M}\mathbf{x} \geq 0\} \tag{11}$$

where $\mathcal{M} = \mathbf{C_{\mathcal{F}_1}}^T\mathbf{C_{\mathcal{F}_2}}\alpha + \mathbf{C_{\mathcal{F}_2}}^T\mathbf{C_{\mathcal{F}_2}}$
with $\mathbf{C_{\mathcal{F}_1}} = [-\mathbf{C}_p\ \mathbf{0}_2\ \mathbf{C}_1]$ and $\mathbf{C_{\mathcal{F}_2}} = [\mathbf{0}_{np}\ 0\ -k_i\rho_r\ \mathbf{0}_{n1}]$.

C. Robustness against sensor noise and stability

The reset control system (8) trivially satisfies the so-called basic hybrid conditions ([29]), since the flow and jump maps are continuous and the sets $\mathcal{F}$ and $\mathcal{J}$ are closed. This gives us some desirable properties like robustness against sensor noise, and also robustness in stability ,see [29] for detailed results.

In this work, the stability analysis is based on [30]; and according to it, the stability notion is pre-input to state stability (pre-ISS). Since developing an ISS Lyapunov function which can verify the stability of the system can be cumbersome in the case of hybrid systems like reset controllers, in [30] a nice frequency domain based stability result is proposed.

The Fig.4 shows the feedback interconnection of a dynamical system ($\mathcal{H}$), shown in Fig.3, and the CI controller. The system $\mathcal{H}$ includes all the linear part of the reset control shown in the highlighted region (orange) in Fig.3 with $\mathbf{w}_1 = r$. The system is considered minimal with

$$\mathcal{L}\{e\} = \mathcal{G}_{eu}(s)\mathcal{L}\{u_{ci}\} + \mathcal{G}_{ew}(s)\mathcal{L}\{\mathbf{w}_1\} \tag{12}$$

where $\mathcal{G}_{eu}, \mathcal{G}_{ew}$ are the transfer function of the system between e with u_{ci} and $\mathbf{w}_1$ as inputs respectively.

The stability of system can be guaranteed if it satisfies the following criteria [30]:

1) The system matrix $\mathcal{H}$ is Hurwitz, that is its eigenvalues are strictly in the left half plane.
2) The transfer function $\mathcal{G}_{eu(s)}$ as in (12) satisfies

$$\frac{1}{\alpha} + Re(\lim_{w\to\infty} \mathcal{G}_{eu(s)}) > 0 \tag{13}$$

and

$$\frac{1}{\alpha} + Re(\mathcal{G}_{eu(s)}) > 0 \quad \forall w \in \mathbb{R} \tag{14}$$

provided matrices $\mathbf{A}_r, \mathbf{C}_r$ in (1,5) is detectable. Satisfying the above criteria will ensure the existence of a pre-ISS Lyapunov function which is smooth with negative derivative between reset instants and decreases in value after a reset instance.

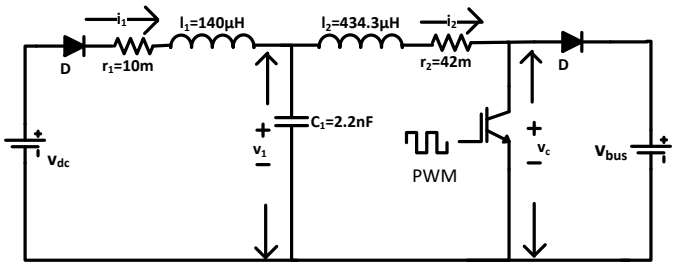

Fig. 5: DC-DC Boost converter schematic with passive components, switching devices and system state voltages, current.

D. Design of PI+CI controller for first order plants

Consider a first order plant P given by

$$P(s) = \frac{b_0}{s + a_0}, \tag{15}$$

subjected to an exogenous input $\mathbf{w}_1$ represented by a step signal of amplitude w_{10}. In [9], it is shown that the closed-loop system error can be forced to zero from the first reset by choosing an appropriate value of ρ_r given by

$$\rho_r = 1 - \frac{a_0 w_{10}}{b_0 k_i x_{i,1}} \tag{16}$$

where $x_{i,1}$ is the value of the integrator state x_i at the first reset instance.

The value for ρ_r defined in (16) is dependant on the nature of exogenous signal applied at the input of the system. The above expression is an optimal value of ρ_r for the step input.

E. Converter modelling

The proposed PI+CI controller can be used in different DC-DC converter topologies. As a first step in this work the implementation is done on a DC-DC boost converter with an input filter shown in Fig.5. The proposed converter is interfacing an ESS or renewable source (v_{dc}) to a DC microgrid. It is assumed that the grid voltage regulation is carried out by another system and that the proposed controller is working in current source mode delivering active power requirements. The inductor l_1 and capacitor c_1 in Fig.5 form the input filter to the DC source, v_{dc}. The inductor l_2 enables the boosting of input voltage to the output (v_{bus}). The resistors r_1 and r_2 are the effective series resistance of inductors l_1 and l_2 respectively. PI controllers have been widely employed for the control of these converters. A drawback can be when tuning these controllers for a fast response, which will lead to large overshoots. This may be overcome with the PI+CI which is capable of producing fast flat response making it suited for DC-DC converters in grid connected systems.

The modelling of the converter is done taking the averaged model of the system by neglecting the high frequency switching ripples. The average voltage across the switch (MOSFET, IGBT) is taken to achieve the same. The average voltage is defined as $v_c = d' v_{bus}$ where $d' = 1 - d$ with d, the duty ratio of the gate signals. The domain of modelling the converters has been subject to extensive research [31]. The converter model for the system shown in Fig.5 is given by (17) (see above).

TABLE I: Component value used in DC-DC converter

Component name	Value
l_1	140 µH
l_2	434.3 µH
c_1	2.2nF
r_1	10mΩ
r_2	42mΩ

A variable change is proposed for (17) as shown below

$$V_{m2}(s) = \frac{V_{dc}(s)}{l_1 c_1 s^2 + r_1 c_1 s + 1} - V_c(s) \tag{18}$$

resulting in a model given by (19) (see above) which will be used for controller design. This variable change is important to ensure that at start up the voltage v_c is same as v_{dc} thereby eliminating large in-rush currents which can be detrimental to the converter components and the power electronic switches.

III. Controller design

The PI+CI control can ensure a fast flat response as shown in the previous section for first order systems. The DC-DC boost converter in Fig.5 though, is a third order system (19) and forcing such a system to have a flat response will be difficult if not impossible with PI+CI controller. Therefore, the original system represented by the converter needs to be reduced so that the system seen by the reset controller is effectively first order. The third-order system presented by the converter is reduced to an effective first order system (P_{red} bounded by the dotted region in Fig.6) using a filter, $F(s)$, designed to have zeros to cancel complex conjugate poles of the converter and poles to cancel the complex conjugate zeros. The Fig.6 is the schematic of the equivalent control system. The converter represented by (19) for the component values shown in Table.I is represented as

$$G(s) = \frac{i_2(s)}{v_{m2}(s)} = \frac{s + 35.70 \pm 1800i}{(s + 87.1)(s + 38.20 \pm 2070i)} \tag{20}$$

the filter F(s) will therefore be:

$$F(s) = \frac{s + 38.20 \pm 2070i}{s + 35.70 \pm 1800i} \tag{21}$$

ensuring a pole zero compensation resulting in P_{red} given by

$$P_{red}(s) = G(s) \cdot F(s) = \frac{1742}{s + 87.1}. \tag{22}$$

This P_{red} is now considered for the calculation of ρ_r for the controller and will be the effective first order system seen by the controller as in (15). The design of the $PI+CI$ is then carried out as follows. First, the PI_{base} parameters k_p and k_i have to be calculated. A base selection of these parameters were carried out using the AMIGO design technique outlined in [32]. The parameters of this base design was then tuned to improve the system performance towards noise entering through plant input as the AMIGO design considers only output noise. This was done since in the DC-DC converter switching noise is introduced at the plant input by converting the control action u in Fig.6 to 20 kHz gate pulses for controlling the IGBTs to achieve the desired output current. A set of PI_{base} parameters where considered and the one with

$$i_2(s) = \frac{v_{dc}(s) - (c_1 l_1 s^2 + c_1 r_1 s + 1) v_c(s)}{l_1 l_2 c_1 s^3 + c_1(l_1 r_2 + l_2 r_1) s^2 + (c_1 r_1 r_2 + l_1 + l_2) s + (r_1 + r_2)} \tag{17}$$

$$G(s) = \frac{i_2(s)}{v_{m2}(s)} = \frac{c_1 l_1 s^2 + c_1 r_1 s + 1}{l_1 l_2 c_1 s^3 + c_1(l_1 r_2 + l_2 r_1) s^2 + (c_1 r_1 r_2 + l_1 + l_2) s + (r_1 + r_2)} \tag{19}$$

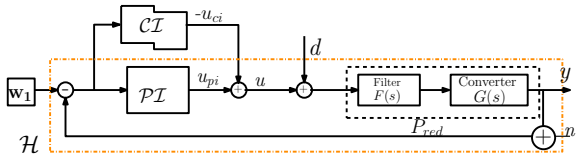

Fig. 6: The closed loop representation of the reset control system employed for the boost converter

better performance in the real DC-DC converter set up was chosen. As the design of a PI_{base} is not the main objective of this work the detailed analysis of the same is not provided for the sake of brevity.

The k_p and k_i values where calculated to be 0.03316 and 19.39 respectively for a settling time of 0.055s.

The fast settling time though results in a peak overshoot of 28%. The next step is to calculate the value of ρ_r using (16) to obtain the flat response. The $k_i x_{i,1}$ term in (16) is the output of the PI_{base} integrator at the instance of first zero crossing of system error. The value for $k_i x_{i,1}$ was calculated off-line using a model of system controlled by PI_{base} and used in the calculation of ρ_r. This resulted in a value of $\rho_r = 0.4889$.

The Fig.7 shows the simulation of reference tracking performance of the plant controlled by the PI_{base} and $PI + CI$ controllers. The effect of the reset controller on improving the tracking performance is clearly observable by the flat response that it produces. The experimental implementation of the same will be discussed in Section.IV.

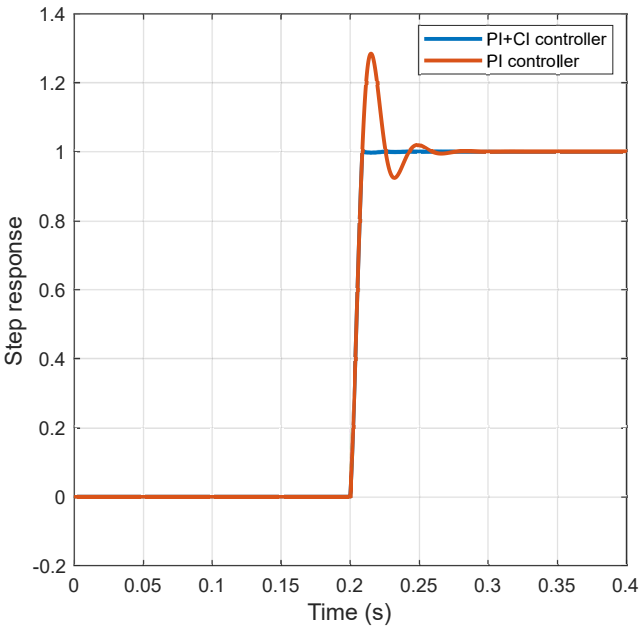

Fig. 7: A comparison in simulation for the step response of the linear PI (orange) and the reset $PI+CI$ (blue) controllers showing the flat response that can be achieved

.

A. *Stability analysis*

Stability of the DC-DC boost converter control system is analysed using the results in Section II.D. In the case of $PI + CI$ controller employed for boost converter in this work, the transfer function $\mathcal{G}_{eu}(s)$ is

$$\mathcal{G}_{eu}(s) = \frac{P_{red(s)}}{1 + P_{red(s)} PI(s)} = \frac{1742s}{s^2 + 144.9s + 33780}. \tag{23}$$

The first criteria of the stability condition will be satisfied by designing a stabilizing PI_{base} such that the linear system represented by $\mathcal{H}$ is stable which is also the case here. The transfer function $\mathcal{G}_{eu}(s) \to 0$ as $w \to \infty$ is trivial thereby, satisfying (13). Finally the fulfilment of (14) is explained through Fig.8. This shows the Nyquist plot of the transfer function $\mathcal{G}_{eu}(s)$. The sector condition for CI controller is defined for $\alpha \to \infty$ resulting in the $Re(\mathcal{G}_{eu(s)})$ to lie on the right half side of the complex plane in the Nyquist plot to ensure condition 2. This can be observed in Fig.8. As a

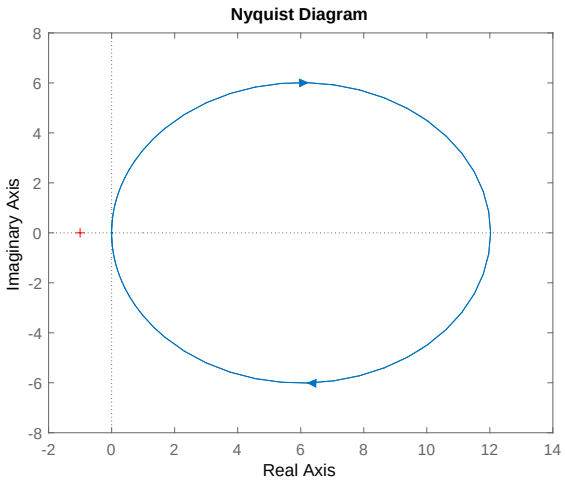

Fig. 8: Nyquist plot for the transfer function $\mathcal{G}_{eu}(s)$

.

result, it is shown that closed-loop system is stable according

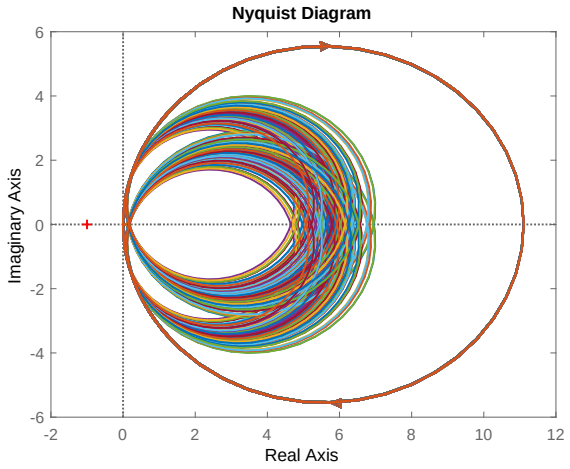

Fig. 9: Nyquist plots of $\mathcal{G}_{eu}(s)$ for the varying values of of boost converter parameters l_1, l_2, c_1

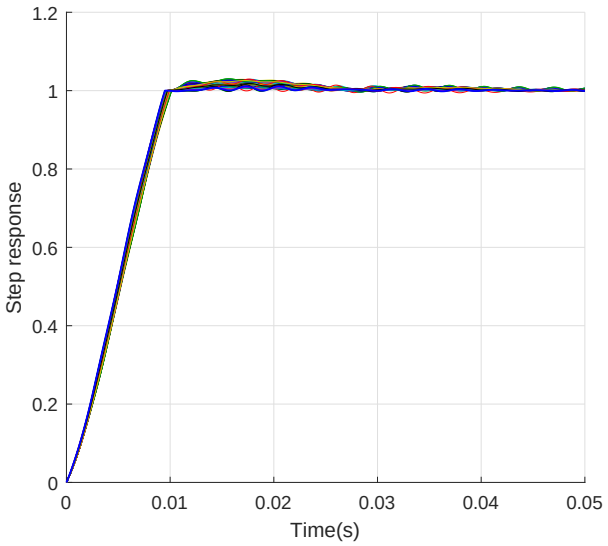

Fig. 10: Step responses of the designed system for parameter variations in l_1, l_2, c_1 for the designed value of $\rho_r = 0.4889$

to Section II.D.

The $PI + CI$ controller used in this work is a hybrid controller and unlike linear systems robustness analysis may not be straightforward. Well-posedness of the reset control systems, as well as robustness to measurement noise and stability easily follow by using the formal methods developed in [29]. The sense of robustness in [29] is related with keeping a desired property, e. g. stability, for arbitrarily small values of for example sensor noise. It is also interesting to analyze if the stability is kept when there exist some parameter uncertainty, which is also a basic issue in control practice. An additional advantage of frequency domain analysis it that it easily allows this type of robustness analysis. An analysis is done in the form of controller performance towards parameter uncertainty. The values of inductors and capacitors are usually mentioned within a range defined as a percentage of the nominal value. Under such conditions an exact pole zero cancellation may not be possible and the system may not be exactly first order. The stability of the system under such scenario needs to be ascertained. The uncertainty in the nominal value of the components l_1, l_2 and c_1 considered here is 10%, based on the data-sheet of these components. The stability under uncertainty is ascertained using the results of Section II.D. Satisfying first condition of stability criteria and (13) is trivial. The effect of uncertainty on the condition (14) is highlighted in Fig.9. The plot in Fig.9 is generated using 100 random values of the components l_1, l_2 and c_1 within the uncertainty range. It can be noted despite the uncertainty the Nyquist plots are always positioned on the right half plane of the complex plane ensuring that (14) is always satisfied thereby establishing stability despite uncertainty. The same is highlighted in Fig.10. This figure shows the step response of the reset controller based boost converter system taking 100 random samples within the uncertainty range.

B. Describing function analysis

Having already established closed loop stability of the system in Section II.D the analysis in this section allows a heuristic understanding of the reset system robustness in comparison to linear base system using describing function (DF), which will be otherwise impossible by any other means. Although, an approximated analysis in control practice it gives an adequate characterization of both stability margins and sensor noise effect, since the feedback loop has the necessary low-pass property. In this context DF analysis can present itself as a simple tool for a designer to provide an intuition on the robustness of the reset control designed using well established frequency domain techniques. Whilst DF analysis have been found to fail in some cases it can still be an important tool and its use in non-linear systems have been justified through the works in [33]–[35].

The describing function of a $PI + CI$ is given by [11]

$$PI + CI(\omega) = k_p \frac{j(w\tau_i + \frac{4}{\Pi}\rho_r) + 1}{j\omega\tau_i} \tag{24}$$

where $\tau_i = \frac{kp}{ki}$. The important characteristic of DF of the $PI + CI$ controller is that the function does not depend on the amplitude of the input but solely on the frequency of input. This allows the use of frequency domain analysis tools in analysing the robustness of reset controllers.

The $PI + CI$ controller has been proposed to overcome the inherent limitation of its linear counterparts. Nevertheless it is necessary to investigate whether this is achieved without increasing the cost of feedback (sensitivity to sensor noise) or sensitivity to load disturbance so that its application is justified. An understanding of this can be achieved using the system transfer functions mentioned in [36], which can be constructed using the DF of $PI + CI$ given by (24). The four system transfer functions considered for the same, mentioned in [36], are system transfer function (TF), sensitivity function (S), noise sensitivity function (CS) and load sensitivity function

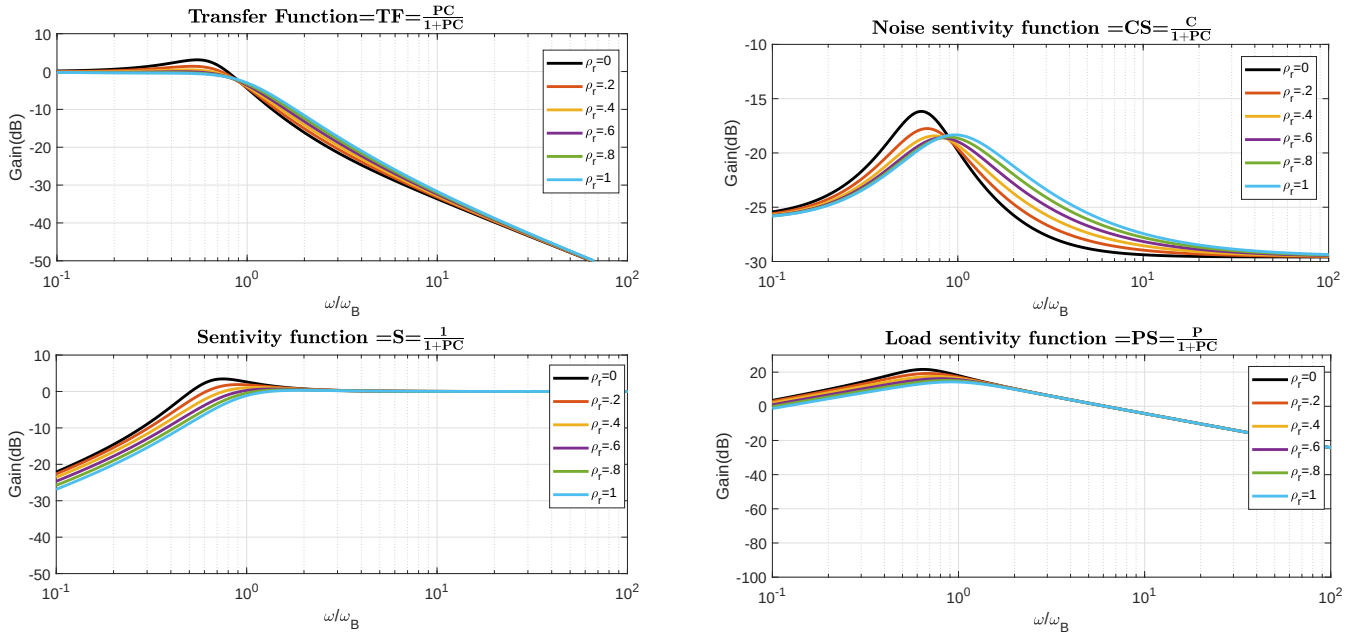

Fig. 11: Bode plots of the system transfer function including closed loop transfer function (TF), Noise sensitivity Function (CS), sensitivity function (S) and load sensitivity function (PS) plotted for linear base system $(\rho_r) = 0$ and for different reset ratios.

(PS) given by

$$TF = \frac{Y(w)}{w_1(w)} = \frac{PI + CI(w) \cdot P_{red}(jw)}{1 + PI + CI(w) \cdot P_{red}(jw)} \tag{25}$$

$$S = \frac{Y(w)}{N(w)} = \frac{1}{1 + PI + CI(w) \cdot P_{red}(w)} \tag{26}$$

$$CS = \frac{U(w)}{N(w)} = \frac{PI + CI(w)}{1 + PI + CI(w) \cdot P_{red}(w)} \tag{27}$$

$$PS = \frac{U(w)}{N(w)} = \frac{P_{red}(w)}{1 + PI + CI(w) \cdot P_{red}(w)}. \tag{28}$$

The Fig.11 shows Bode plots of eqs. (25) to (28) for varying values of ρ_r. The frequency axis is normalised using the cut-off frequency w_b. It can be observed from Fig.11 that the system reference to output transfer function (TF) gains are very similar for the linear ($\rho_r = 0$) and reset system for the entire frequency range. The linear system though will exhibit an higher overshoot compared to reset system based on the plots which is to be expected as the reset action ensures flat response. The closed loop bandwidth remains the same ($w/w_b = 1$) and the reset system performance is very similar to the base system at high frequencies. The DC/DC converter presented in this work is a system where the noise will enter through the plant input d (Fig.6) in the form of switching noise. The continuous time control input u will be converted to 20 kHz gate pulses for the IGBTs using pulse width modulation (PWM). Therefore an interesting plot to study will be the effect of plant output to noise input d which is given by load sensitivity function (PS). This also allows understanding of load disturbance rejection capability of the plant. It can be seen from Fig.11 that the addition of reset action has actually reduced the sensitivity of the system towards input disturbance. Nevertheless at switching frequency of 20 kHz the

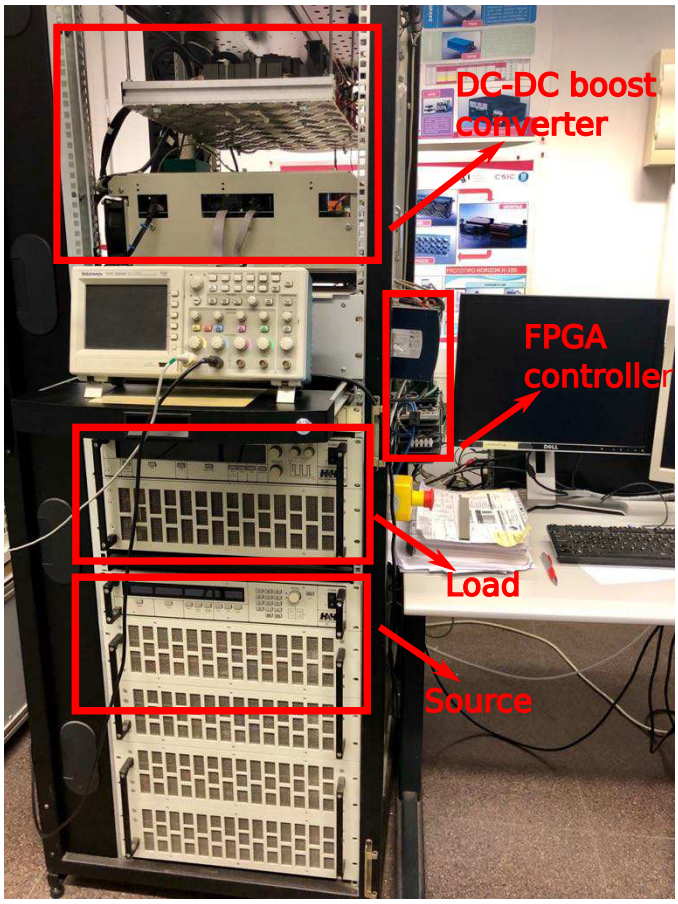

Fig. 12: Laboratory setup of the DC-DC boost converter with programmable source and sinks

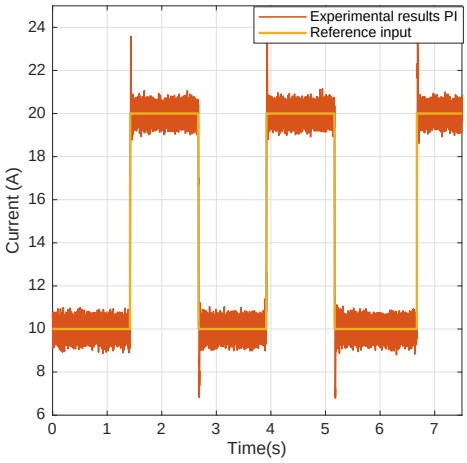

Fig. 13: Reference tracking performance of the converter (red) when used with PI_{base} controller for reference input (orange). The overshoot with PI_{base} controller can be observed here.

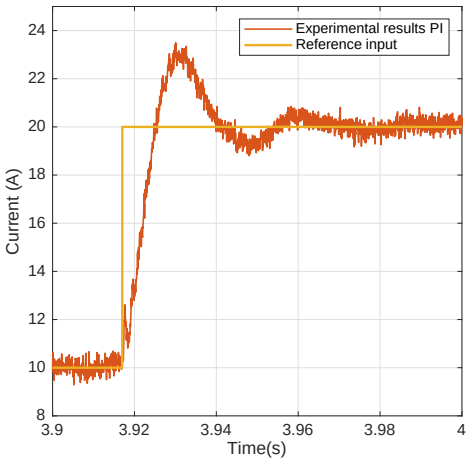

Fig. 14: Zoom in near a rising edge of the step response in Fig.13 highlighting the overshoot resulting from PI_{base} controller

gain plots are same showing similar performance. Finally, the effect of measurement (output) noise on the plant performance is studied through the noise sensitivity (CS) and sensitivity (S) functions.The linear base system still exhibits a higher sensitivity in comparison to the reset systems. It should also be noted that in all the above functions higher the reset ratio lesser is the sensitivity of the function. Therefore a general consensus that can be drawn from here is that the reset action does improve the system performance by producing a fast flat response and provides a marginal improvement in system robustness observed by reduced gains in the sensitivity functions. This is still a heuristic understanding and may not be truly reflective of the actual system performance. The real impact of the reset system will be discussed in the next section where results from an actual converter system subjected to measurement and switching noises will be presented.

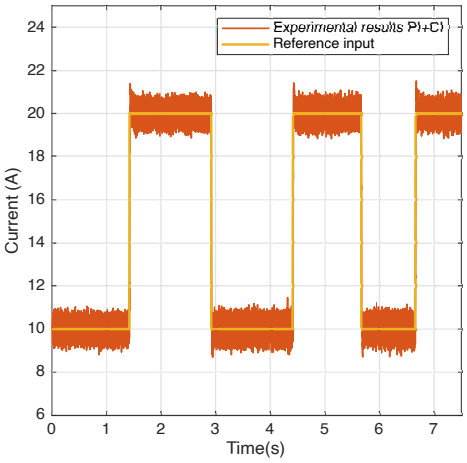

Fig. 15: Reference tracking performance of converter set up (red) when used with $PI + CI$ reset controller. The flatter response from reset control is observed.

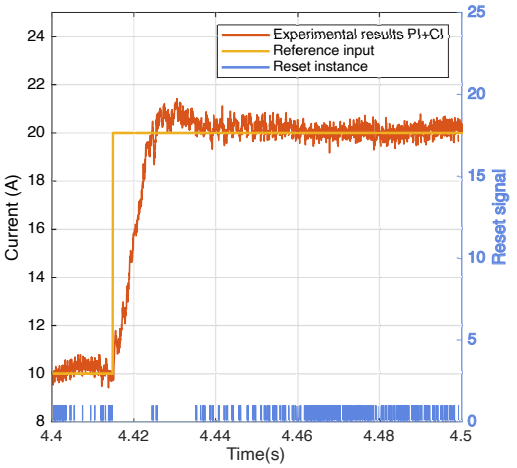

Fig. 16: Zoom in at rising edge of the step response from Fig.15 emphasizing the flat trajectory achieved with reset control and the reset instances (blue).

IV. Implementation and Results

The Fig.12 shows the laboratory set up where the proposed $PI + CI$controller was implemented. The DC-DC converter uses IGBT modules from Semikron. The Höcherl & Hackl NL series programmable source/sink was used as input DC source and DC grid was emulated through the Höcherl & Hackl ZS series electronic load. The controller was implemented in FPGA (CompactRIO from NI) using LabVIEW.

The Fig.13 shows tracking performance of the converter under a varying reference alternating between 10A and 20 A when used with PI_{base} (fast PI) controller. The higher overshoot which arises at converter output due the fast PI action from the PI_{base} controller can be noticed in Fig.13 and is emphasised in Fig.14 where the rising edge of the step response is zoomed into. These overshoots when injected into weak grids can cause voltage variations beyond permissible limit. It is this overshoot which can be negated with well designed reset control.

The Fig. 15 shows reference tracking of the converter when using the $PI + CI$ controller under a reference value alternating between 10A and 20A. In comparison to Fig.13 the tracking performance under $PI + CI$ is devoid of overshoots as shown in Fig.15 when subjected to step change in reference value. The absence in overshoot is clearly observed in Fig.16 where the response in Fig.15 is zoomed at a rising edge. The peak value at the transient period for the $PI + CI$ controller based system shows almost 10 % reduction in comparison to that of the PI controller in Fig.14. The Fig.16 also presents reset signals (violet) which resets the CI at the lower portion of figure. It should also be noted the settling time of the response is faster in the $PI+CI$ controller based system in comparison to the linear system as can be seen from Fig.14 and Fig.16.

It is observed that the plot of converter response in Fig.13 and Fig.15 when using both PI and $PI + CI$ controller appears noisy. This is contributed mainly by the measurement noise of high bandwidth Hall sensors used in the current measurement. The effect of measurement noise on the reset action is observable in Fig.16 through the reset signals. The noise corrupted signal used in FPGA causes the CI implemented in it to be reset multiple times during steady state condition as evident by the large number of reset signals in Fig.16. Nevertheless it should be noted that the reset signals are well posed (well-defined and are distinct). It should also be noted that the effect of noise inherent to the hall sensor has negligible impact on the stability of the system as evident by the response of PI+CI controller based system in Fig.15 highlighting robustness of the proposed technique under measurement noise.

V. Conclusion

The PI+CI controller implemented for the DC-DC boost converter has exhibited improved performance over a well designed PI controller by achieving a flat response. The design of this controller has been relatively straight forward using simple analytical equations and enables easy implementations. In terms of complexity in implementing the same controller in FPGA there is not much increase over the PI_{base} as it simply involves adding an integrator in parallel, which resets at the zero crossings of the error signal. Overall, it can be concluded that the $PI + CI$ reset controller provides better performance without increasing the complexity in terms of design, implementation and sensitivity to sensor noise. These converters capable of producing flat fast responses can find increased application in grid connected systems to respond to sudden load changes without creating much deviations from the prescribed nominal values.

In terms of future work there are many issues which can be addressed, the most important being the disturbance rejection capabilities of these controllers especially for converters which are employed in hybrid system applications like the electric grids.

References

[1] J. C. Clegg, "A nonlinear integrator for servomechanisms," *Transactions of the American Institute of Electrical Engineers, Part II: Applications and Industry*, vol. 77, no. 1, pp. 41–42, 1958.

[2] K. R. Krishnan and I. M. Horowitz, "Synthesis of a non-linear feedback system with significant plant-ignorance for prescribed system tolerances," *International Journal of Control*, vol. 19, no. 4, pp. 689–706, apr 1974.

[3] I. Horowitz and P. Rosenbaum, "Non-linear design for cost of feedback reduction in systems with large parameter uncertainty," *International Journal of Control*, vol. 21, no. 6, pp. 977–1001, 1975.

[4] L. Zaccarian, D. Nešić, and A. R. Teel, "Analytical and numerical lyapunov functions for siso linear control systems with first-order reset elements," *International Journal of Robust and Nonlinear Control*, vol. 21, no. 10, pp. 1134–1158, 2011.

[5] L. Zaccarian, D. Nesic, and A. R. Teel, "First order reset elements and the clegg integrator revisited," in *Proceedings of the 2005, American Control Conference, 2005.*, June 2005, pp. 563–568 vol. 1.

[6] D. Nesic, A. R. Teel, and L. Zaccarian, "Stability and performance of siso control systems with first-order reset elements," *IEEE Transactions on Automatic Control*, vol. 56, no. 11, pp. 2567–2582, Nov 2011.

[7] A. Baños and A. Barreiro, "Delay-independent stability of reset systems," *IEEE Transactions on Automatic Control*, vol. 54, no. 2, pp. 341–346, 2009.

[8] A. Baños and A. Vidal, "Design of Reset Control Systems: The PI+CI Compensator," *Journal of Dynamic Systems, Measurement, and Control*, vol. 134, no. 5, p. 051003, 2012.

[9] A. Baños and M. Davó, "Tuning of reset proportional integral compensators with a variable reset ratio and reset band," *IET Control Theory and Applications*, vol. 8, no. 17, pp. 1949–1962, 2014.

[10] O. Beker, C. V. Hollot, and Y. Chait, "Plant with integrator: an example of reset control overcoming limitations of linear feedback," *IEEE Transactions on Automatic Control*, vol. 46, no. 11, pp. 1797–1799, Nov 2001.

[11] A. Baños and A. Barreiro, *Reset control systems*. Springer Science & Business Media, 2012.

[12] A. Baños, J. I. Mulero, A. Barreiro, and M. A. Davo, "An impulsive dynamical systems framework for reset control systems," *International Journal of Control*, vol. 89, no. 10, pp. 1985–2007, 2016.

[13] J. Carrasco, A. Baños, and A. van der Schaft, "A passivity-based approach to reset control systems stability," *Systems & Control Letters*, vol. 59, no. 1, pp. 18–24, 2010.

[14] A. F. Villaverde, A. B. Blas, J. Carrasco, and A. B. Torrico, "Reset control for passive bilateral teleoperation," *IEEE Transactions on Industrial Electronics*, vol. 58, no. 7, pp. 3037–3045, July 2011.

[15] A. Vidal, A. Baños, J. C. Moreno, and M. Berenguel, "Pi+ci compensation with variable reset: Application on solar collector fields," in *2008 34th Annual Conference of IEEE Industrial Electronics*, Nov 2008, pp. 321–326.

[16] M. F. Heertjes, K. G. J. Gruntjens, S. J. L. M. van Loon, N. van de Wouw, and W. P. M. H. Heemels, "Experimental Evaluation of Reset Control for Improved Stage Performance," *IFAC-PapersOnLine*, no. 13, pp. 93–98, 2016.

[17] A. Vidal and A. Baños, "Reset compensation for temperature control: Experimental application on heat exchangers," *Chemical Engineering Journal*, vol. 159, no. 1-3, pp. 170–181, 2010.

[18] J. M. Carrasco, L. G. Franquelo, J. T. Bialasiewicz, E. Galvan, R. C. PortilloGuisado, M. A. M. Prats, J. I. Leon, and N. Moreno-Alfonso, "Power-electronic systems for the grid integration of renewable energy sources: A survey," *IEEE Transactions on Industrial Electronics*, vol. 53, no. 4, pp. 1002–1016, June 2006.

[19] B.-R. Lin and Y.-C. Huang, "Bidirectional dc converter with frequency control: Analysis and implementation," *Energies*, vol. 11, no. 9, 2018.

[20] H. Bory Prevez, H. Martinez Garcia, L. Vazquez Seisdedos, F. Chang Muman, and L. Alfredo Enriquez Garcia, "Comparacin entre rectificador trifsico con conmutacin simtrica y convertidor ac/ac para la mejora del factor de potencia en microcentrales hidroelctricas," *Revista Iberoamericana de Automtica e Informtica industrial*, vol. 15, no. 1, pp. 101–111, 2017.

[21] K. Divya and J. Østergaard, "Battery energy storage technology for power systemsan overview," *Electric Power Systems Research*, vol. 79, no. 4, pp. 511 – 520, 2009.

[22] P. Denholm, E. Ela, B. Kirby, and M. Milligan, "The role of energy storage with renewable electricity generation," 2010.

[23] R. S. Ashok and Y. B. Shtessel, "Sliding mode control of electric power system comprised of fuel cell and multiple-modular dc-dc boost converters," in *2014 13th International Workshop on Variable Structure Systems (VSS)*, June 2014, pp. 1–7.

[24] R. S. Ashok, Y. B. Shtessel, and J. E. Smith, "Sliding mode control of electric power system comprised of fuel cells, dc-dc boost converters

and ultracapacitors," in *2013 American Control Conference*, June 2013, pp. 5766–5771.
[25] V. Ramanarayanan, "Sliding mode control of power converters thesis," *PhD thesis*, 1986.
[26] P. Thounthong, P. Tricoli, and B. Davat, "Performance investigation of linear and nonlinear controls for a fuel cell/supercapacitor hybrid power plant," *International Journal of Electrical Power and Energy Systems*, vol. 54, pp. 454–464, 2014.
[27] U. R. Nair, R. Costa-Castelló, and A. Baños, "Reset control of boost converters," in *2018 Annual American Control Conference (ACC)*. IEEE, 2018, pp. 553–558.
[28] O. Beker, C. Hollot, Y. Chait, and H. Han, "Fundamental properties of reset control systems," *Automatica*, vol. 40, no. 6, pp. 905 – 915, 2004.
[29] R. Goebel, R. G. Sanfelice, and A. R. Teel, *Hybrid Dynamical Systems: modeling, stability, and robustness*. Princeton University Press, 2012.
[30] S. van Loon, K. Gruntjens, M. Heertjes, N. van de Wouw, and W. Heemels, "Frequency-domain tools for stability analysis of reset control systems," *Automatica*, vol. 82, pp. 101–108, 2016.
[31] R. W. Erickson, *Fundamentals of Power Electronics Fundamentals of Power Electronics*. Kluwer Academic, 2002.
[32] T. Hägglund and K. J. Åström, "Revisiting the ziegler-nichols tuning rules for pi control," *Asian Journal of Control*, vol. 4, no. 4, pp. 364–380, 2002.
[33] A. Bergen and R. Franks, "Justification of the describing function method," *SIAM Journal on Control*, vol. 9, no. 4, pp. 568–589, 1971.
[34] A. Mees and A. Bergen, "Describing functions revisited," *IEEE Transactions on Automatic Control*, vol. 20, no. 4, pp. 473–478, August 1975.
[35] S. R. Sanders, "On limit cycles and the describing function method in periodically switched circuits," *IEEE Transactions on Circuits and Systems I: Fundamental Theory and Applications*, vol. 40, no. 9, pp. 564–572, Sept 1993.
[36] K. J. Aström and R. M. Murray, *Feedback systems: An introduction for scientists and engineers*. Princeton university press, 2010.